Elastic constants and electronic structure of fluorite (CaF_2): an ab initio Hartree-Fock study

1991 J. Phys.: Condens. Matter 3 4151

(http://iopscience.iop.org/0953-8984/3/23/004)

J. Phys.: Condens. Matter 3 (1991) 4151–4164. Printed in the UK

Elastic constants and electronic structure of fluorite (CaF_2): an *ab initio* Hartree–Fock study

M Catti†, R Dovesi‡, A Pavese§ and V R Saunders¶

† Department of Physical Chemistry and Electrochemistry, University of Milano, via Golgi 19, I–20133, Italy
‡ Department of Inorganic, Physical and Materials Chemistry, University of Torino, via Giuria 5, I–10125, Italy
§ Department of Earth Sciences, Section of Mineralogy and Crystallography, University of Torino, via V. Caluso 37, I–10125 Torino, Italy
¶ Daresbury Laboratory, Science and Engineering Research Council, Daresbury, Warrington WA4 4AD, UK

Received 12 November 1990

Abstract. The ground state properties of fluorite (CaF_2) have been studied using CRYSTAL, an *ab initio* periodic Hartree–Fock program. Twenty-two and thirteen atomic orbitals (represented as contracted Gaussian-type functions) are used for the calcium and fluorine atoms, respectively. The binding energy (BE), the equilibrium lattice parameter (a), the elastic constants (C_{ij}) and the central zone phonon frequencies ν(IR) and ν(Raman) have been evaluated, and a good agreement obtained with experiment (for instance the error is +2.0, +1.7, −0.5% for BE, a and C_{11}, respectively). The calculated C_{44} elastic constant reduces from 48 to 44 GPa (experimental value: 37 GPa) when the fluorine atoms are allowed to displace under strain, indicating the importance of inner deformation for shear elasticity. Electron density maps, density of states and band structure plots are reported which confirm the fully ionic nature of fluorite.

1. Introduction

The elastic constants and phonon dispersion curves of ionic crystals have usually been calculated by classical methods based on Born-type semi-empirical formulae for the interatomic potential energy, usually supplemented by the dipole shell model (Dick and Overhauser 1958), and less frequently by the breathing shell model (Woods *et al* 1960, Schröder 1966, Nusslein and Schröder 1967, Basu and Sengupta 1968) or quadrupolar shell model (Fischer *et al* 1972, Fischer 1974). More recently the electron-gas approximation (Gordon and Kim 1972) has been applied either straightforwardly (Cohen and Gordon 1976, Muhlhauser and Gordon 1981a) or in the 'potential induced breathing' form (Muhlhauser and Gordon 1981b, Hemley *et al* 1985, Mehl *et al* 1986, Cohen *et al* 1987, Jephcoat *et al* 1988, Feldman *et al* 1988) to the alkali halides and alkaline-earth oxides, while the local density functional approach has also recently found application (Melvin and Hendry 1982, Chang and Cohen 1984, Froyen and Cohen 1984, Christensen 1986, Feldman *et al* 1987, Mehl *et al* 1988, Chen *et al* 1988). Also of interest are applications of elementary tight-binding theory (Straub and Harrison 1989). Recent advances in the speed and accuracy of the Hartree–Fock

0953-8984/91/234151+14$03.50

computer program CRYSTAL (Pisani *et al* 1988, Dovesi *et al* 1989) now permit realistic applications of the Hartree–Fock method for the computation of potential energy surfaces in solids point by point, as a function of the appropriate lattice deformations or atom displacements; suitable second derivatives of the energy are then calculated numerically with respect to strain components or atom positions, to yield theoretical values for the elastic constants or phonon frequencies respectively. This possibility is explored with respect to fluorite (CaF_2) in the present work.

Fluorite CaF_2 is cubic $Fm3m$ with four formula units in the unit cell, and represents a very important structure type for several metal halides, oxides and sulphides, and for many intermetallic compounds (Wyckoff 1968). The interest in a number of these solids for their point-defect properties is well known, together with the related peculiar optical behaviour and large ionic conductivity. Previous quantum studies of CaF_2 concerned its electron band structure by a tight-binding method (Albert *et al* 1977) or by a CNDO approximation (Evarestov *et al* 1989), but lattice and elastic properties were not considered. Calculations of the elasticity data of fluorite have been performed by Born-type classical methods (Catlow and Norgett 1973, Catlow *et al* 1978).

Following previous work on MgO (Causa' *et al* 1986), where only the bulk elastic modulus was computed, a full study of the elastic properties and the electron band structure of CaF_2 by the *ab initio* HF-LCAO approach is presented here.

2. Method of calculation and basis set

The all-electron *ab initio* self-consistent-field (SCF) HF-LCAO computational scheme, as implemented in CRYSTAL (Dovesi *et al* 1989) has been previously described (Pisani *et al* 1988). We simply remark here that CRYSTAL is a general program for the treatment of crystalline compounds of any space group, which may be applied to the study of crystals, slabs and polymers. The ionic crystals LiH (Dovesi *et al* 1984a), Li_2O (Dovesi 1984), Li_3N (Dovesi *et al* 1984b) and MgO (Causa' *et al* 1986) have been studied. Recent improvements in the accuracy and speed of the program now allow the evaluation of elastic constants and central zone phonon frequencies (these were not considered in previous studies), by computing numerically the second derivatives of the energy.

There are three possible sources of errors in the present approach. The first is related to the numerical accuracy with which the total energy for a given configuration is calculated. Approximations are introduced in evaluating the infinite Coulomb and exchange series which contribute to the Fock matrix, as well as in the reciprocal space integration required for the SCF cycle (Pisani *et al* 1988, Orlando *et al* 1990). In the present case the computational parameters which control these approximations could be adjusted so that the uncertainties propagated to the calculated binding energy (BE), equilibrium lattice parameter (a) and elastic constants (C_{ij}), are estimated to be of the order of 0.3, 0.1 and 0.5%, respectively.

A second source of error is related to the finite size of the variational basis set. The basis set adopted for the present calculations is reported in table 1. Twenty-two 'atomic orbitals' have been used for calcium, and thirteen for fluorine. Each atomic orbital is a linear combination ('contraction') of Gaussian-type functions (GTF), which are the product of a radial Gaussian and a real solid harmonic function. In the notation of Hehre *et al* (1986), the two basis sets are indicated as 8–6–5–11G* and 7–311G,

Table 1. Exponents (Bohr^{-2}) and coefficients of the Gaussian functions adopted for the present study. The contraction coefficients multiply individually normalized Gaussians. $y(\pm x)$ stands for $y \times 10^{\pm x}$.

Shell type	Calcium			Fluorine		
	Exponents	Coefficients		Exponents	Coefficients	
		s	p or d		s	p
1s	1.913(+5)	2.204(−4)		1.377(+4)	8.77(−4)	
	2.697(+4)	1.925(−3)		1.590(+3)	9.15(−3)	
	5.696(+3)	1.109(−2)		3.265(+2)	4.86(−2)	
	1.489(+3)	4.995(−2)		9.166(+1)	1.691(−1)	
	4.483(+2)	1.701(−1)		3.046(+1)	3.708(−1)	
	1.546(+2)	3.685(−1)		1.15(+1)	4.165(−1)	
	6.037(+1)	4.034(−1)		4.76	1.306(−1)	
	2.509(+2)	1.452(−1)				
2sp	4.486(+2)	−5.75(−3)	8.47(−3)	1.9(+1)	−1.094(−1)	1.244(−1)
	1.057(+2)	−7.67(−2)	6.027(−2)	4.53	−1.289(−1)	5.323(−1)
	3.469(+1)	−1.122(−1)	2.124(−1)	1.37	1.0	1.0
	1.35(+1)	2.537(−1)	3.771(−1)			
	5.82	6.88(−1)	4.01(−1)			
	1.819	3.49(−1)	1.98(−1)			
3sp	2.075(+1)	−2.00(−3)	−3.65(−2)	4.5(−1)	1.0	1.0
	8.4	−1.255(−1)	−6.85(−2)			
	3.597	−6.96(−1)	1.57(−1)			
	1.408	1.029(+0)	1.482(+0)			
	7.26(−1)	9.44(−1)	1.025(+0)			
4sp	4.53(−1)	1.0	1.0	1.8(−1)	1.0	1.0
5sp	2.46(−1)	1.0	1.0			
3d	3.191		1.6(−1)			
	8.683(−1)		3.13(−1)			
	3.191(−1)		4.06(−1)			

respectively, where the numbers refer to the level of contraction, and the star indicates the presence of d polarization functions. The exponents and contraction coefficients of these basis sets were fully optimized in parallel studies of CaO and LiF (rock salt structures); the exponents of the most diffuse Gaussian sp shell of both Ca and F have been reoptimized for fluorite in the present work. A critical point in the choice of basis set for CaF_2 is related to the role of d orbitals for the Ca atom. The set of d orbitals represented by a single Gaussian (1G; $\alpha = 0.6$ Bohr^{-2}), or by the 3G contraction reported in table 1, was first considered. Although the population of d orbitals is always quite small (0.10 electrons in both cases), the influence on the structural parameters is far from negligible: the decrease in BE with respect to the calculation with no d orbitals is 0.012 (1G d orbitals) and 0.017 (3G contraction) hartree; the lattice parameter contraction is 0.042 and 0.063 Å, whereas the bulk modulus increases by 4.0 and 6.5 GPa, respectively. A double set of d orbitals (2G and 1G contractions) was also considered; the results for BE, a and B were very close to those obtained with the 3G set of table 1. The sp valence basis set of Ca appears to provide all the required variational freedom. Another critical point of the basis set concerns the representation of fluorine valence electrons; a 7–31G scheme, instead of the more accurate 7–311G of table 1, increases the elastic constants by about 5%. It would be interesting to check the adequacy of the fluorine basis set of table 1 by introducing a third diffuse sp shell (7–3111G). However, the use of very diffuse functions is not compatible with the present structure of CRYSTAL; we can simply guess, on the basis of the trend from 7–31G to 7–311G and by comparison with parallel studies on similar systems, that the effect of additional functions should not be larger than a 3% change in the elastic constants.

The third source of error in the present study is due to the intrinsic limits of the Hartree–Fock approximation. It is well known (Hehre *et al* 1986) from molecular experience that the Hartree–Fock approach underestimates (in covalent systems) the binding energies by about 30%, whereas the bond lengths are overestimated by 0.5–1%. Similar results were obtained in a systematic study devoted to IV–IV and III–V semiconductors (Orlando *et al* 1990). For ionics, the few previous studies seem to confirm this trend, although more experience is required both in terms of explored properties and type of ions considered. As will be shown in the following, the HF binding energy can be easily corrected in order to take into account the correlation contribution.

3. The binding energy

The data used for evaluating the binding energy are reported in table 2. The total crystal energy refers to the basis set of table 1 with the lattice constant at the energy minimum (table 3). The total energy of isolated atoms was computed starting from the crystalline basis. In the case of fluorine the exponents of the two most diffuse sp shells were reoptimized ($\alpha = 0.44$ and 0.15 Bohr^{-2}). For calcium the basis set of table 1, essentially designed to describe an ionic situation, was supplemented by two diffuse sp shells, in order to provide additional variational freedom accounting for the tails of the atomic wavefunction. Exponent optimization of the three most diffuse sp shells led to the values 0.338, 0.118 and 0.036. The difference between crystal and atomic energies is BE (HF), the Hartree-Fock approximation to the binding energy. The electron correlation contribution to the BE was estimated as the difference in the correlation energies between the pairs Ca^{2+}/Ca and F^-/F, the data for isolated atoms and ions being taken from Clementi (1963). In this model all the correlation contribution to BE is ascribed to charge transfer, whereas the contribution from relaxation of the atomic and ionic wavefunctions due to the crystalline field is disregarded.

The experimental value of the BE can be obtained from the formation enthalpy ΔH_f of fluorite at 298 K, by a conventional Born–Haber thermochemical cycle. Cooling metal Ca and gaseous F_2 down to 0 K, sublimation of Ca and dissociation of F_2 molecules are involved (Weast 1987). The zero-point vibrational energy, evaluated by the Debye model ($\Theta_D = 519.4$ K, Ho and Ruoff 1967), was subtracted. Good agreement between calculated and experimental values of the BE can be observed in table 2, with a deviation of 2%; in a similar comparison for MgO with the rock salt structure (Causa' *et al* 1986), the deviation turned out to be 4.6%.

4. Elastic, lattice and vibrational data

Two sets of experimental data for the C_{11}, C_{12} and C_{44} adiabatic elastic constants of fluorite, measured at different temperatures, were considered. From these the bulk

Table 2. HF total energy at equilibrium (per CaF_2 unit formula), atomic energies and binding energy (BE) (hartree). δE is the correlation contributions to BE evaluated from the correlation energy difference between the isolated atoms and ions. $\Delta\%$ is the percentage error with respect to the experimental value BE(exp).

	CaF_2	Ca	F
E (HF)	−875.946307	−676.725795	−99.374016
BE (HF)	−0.472		
$\Delta\%$	+20.14		
Correlation contribution			
δE (ion corr.)	−0.107	0.041	−0.074
BE (HF + ion corr.)	−0.579		
$\Delta\%$	+2.03		
BE (exp.)	−0.5910[a]		

[a] Weast 1987.

Table 3. Unit-cell edge a (Å), bulk modulus B (GPa), elastic constants C_{ij} (GPa) and central zone transverse optical phonon frequencies ν (THz) of CaF_2. All experimental data have been extrapolated to the athermal limit. $\Delta\%$ is the percentage error of the calculated results with respect to experiment.

	Calculated	Experimental		$\Delta\%$	
a	5.538	5.445[a]		+1.7	
C_{11}	172.2	174.8[b]	173.0[c]	−1.5	−0.5
C_{12}	38.6	47.9[b]	40.5[c]	−19.4	−4.7
C_{44}	44.0	37.2[b]	37.5[c]	+18.3	+17.3
B	82.6	90.2[b]	84.7[c]	−8.4	−2.5
$C_{11} - C_{12}$	133.6	126.9[b]	132.5[c]	+5.3	+0.8
$C_{11} + C_{12}$	210.8	222.7[b]	213.5[c]	−5.3	−1.3
ν(Raman)	10.1	9.91[d]		+1.9	
ν(IR)	8.1	8.33[e]		−2.8	

[a] White (1980).
[b] Ultrasonic (Ho and Ruoff 1967).
[c] Brillouin scattering (Catlow *et al* 1978).
[d] Denham *et al* (1970).
[e] Lowndes (1971).

elastic modulus can be derived, according to the relation $B = (C_{11} + 2C_{12})/3$. The first data (Ho and Ruoff 1967) were obtained by ultrasonic measurements between 4 and 295.5 K; the second set (Catlow *et al* 1978) is based on Brillouin scattering experiments at a number of temperatures in the range 300–1500 K. By comparing the two sets of adiabatic C_{11}, C_{12} and C_{44} constants determined at room temperature (165.07, 44.51, 33.83 and 165.5, 38.9, 33.5 GPa for ultrasonic and Brillouin scattering data, respectively), the C_{11} and C_{44} values appear to be consistent, but not those for C_{12}. A parallel discrepancy is transferred to the bulk modulus B (84.7 and 81.1 GPa, respectively). The extra-diagonal elastic constants are well known to be affected by larger measurement errors.

For comparison with the present theoretical results, the experimental elastic constants at the athermal limit have been found by extrapolating back to 0 K the plot of elastic constants against T from the linear region at higher temperature (Liebfried and Ludwig 1961, Garber and Granato 1975a, b). In figure 1 the data of Ho and

Ruoff (1967) are shown, with the extrapolation lines obtained by interpolating the three measurements at 295.5, 273.15 and 194.5 K. An analogous procedure was applied to the high temperature data of Catlow *et al* (1978), obtaining straight lines with similar slopes for the C_{11}, C_{12} and C_{44} constants. In table 3 both sets of results are reported. Similarly, the unit-cell edge at 301 K, $a = 5.463$ Å (Wyckoff 1968) has been extrapolated back to the athermal limit using experimental thermal expansion data (White 1980), to yield the value quoted in table 3.

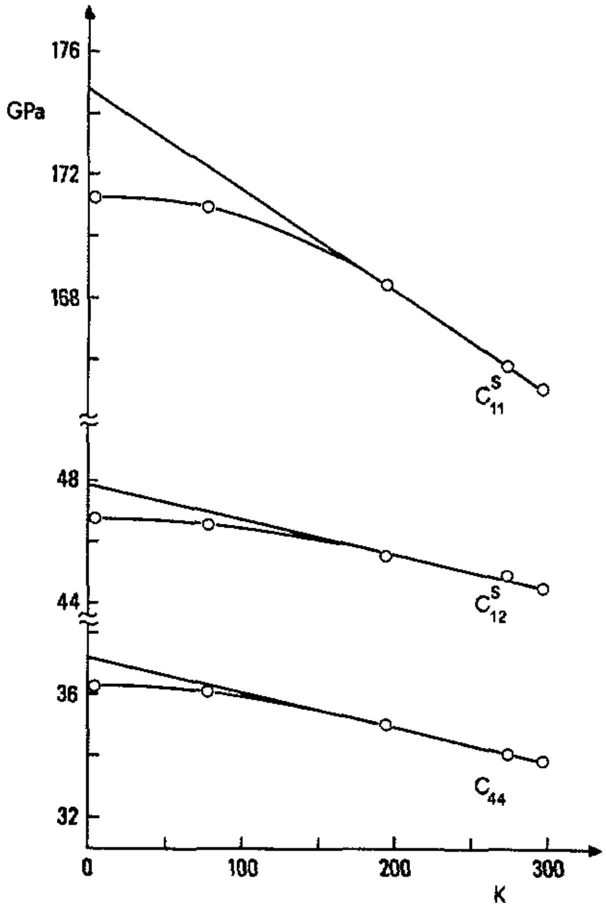

Figure 1. Elastic constants of fluorite measured against temperature (circles) by Ho and Ruoff (1967). Straight lines for extrapolation to 0 K are shown.

By using the atomic orbital basis sets of table 1, the total energy of fluorite was calculated for a number of different deformations of the unit cell. The energy values against strain components η_i were fitted to polynomial functions up to the fourth order. Thus the second derivatives of energy (at the energy minimum) could be calculated and yielded the elastic constants C_{ij}, according to the relation (valid at 0 K):

$$C_{ij} = \frac{1}{V}\left[\frac{\partial^2 E}{\partial\eta_i \partial\eta_j}\right]_0 . \qquad (1)$$

By simply changing the edge a of the cubic unit cell, an isotropic deformation of the crystal structure was attained, which yielded the equilibrium value of a at zero stress (minimum point of energy) and the bulk elastic modulus B (second derivative of the energy at the minimum point). The energy was computed at eight a values in the range 5.40–5.70 Å. Least-squares fits were performed for the $E(a)$ function both to polynomials and to the Murnaghan (1944) equation of state:

$$E(V) = E_0 + \frac{B}{B'}V\left[\frac{1}{B'-1}(V_0/V)^{B'} + 1\right] - \frac{B}{B'-1}V_0 \tag{2}$$

where B' means $\partial B/\partial V$. The equilibrium value of a at the energy minimum (table 3) is practically independent of the interpolation scheme, and B also shows a good stability to variation in the interpolating function; the value reported in table 3 corresponds to the Murnaghan formula.

The calculated cell edge turns out to be larger than that observed by 1.7%, with a positive deviation of 0.093 Å, while a negative deviation appears between computed and experimental B values. A better agreement with the Brillouin scattering than with the ultrasonic data is observed for the bulk modulus. The behaviours of a and B would seem to be consistent with each other, as the larger volume found by the calculation would reasonably imply a less stiff crystal. The results obtained in the calculation of cell edge and bulk modulus for CaF_2 can be compared with the analogous ones for MgO (Causa' *et al* 1986). In the latter case, the computed and measured lattice constants are very close to each other ($\Delta < 0.01$ Å), while the theoretical values of B are larger than the experimental data by about +10%. The much larger error in the calculated lattice parameter for CaF_2 with respect to MgO, LiH and Li_2O is probably related to the large atomic number of Ca, which gives rise to important effects of atomic polarization and electron correlation, not taken into account by the HF model. The better agreement for the bulk modulus is simply a consequence of the larger lattice parameter value, which partially compensate the expected HF overestimation of B.

Values of the linear combinations of elastic constants $C_{11} + C_{12}$ and $C_{11} - C_{12}$ were computed by applying the deformations $[\eta\ \ \eta\ \ 0\ \ 0\ \ 0\ \ 0]$ and $[\eta\ \ \eta\ \ -2\eta\ \ 0\ \ 0\ \ 0]$, respectively. The former corresponds to contracting two of the three edges of the cubic cell by equal amounts, and the latter to contracting two and stretching one edge by a double amount. For each of these deformations, the second derivative of energy needs to be calculated numerically with respect to the single parameter η, as it appears form the second-order expansion of the elastic energy

$$E = \tfrac{1}{2}\sum_{1}^{6}{}_{ij}C_{ij}\eta_i\eta_j. \tag{3}$$

This allows a reduction in the number of CRYSTAL runs with respect to using the straightforward formula (1), which involves the computation of mixed derivatives (Catti 1982). Ten values of η were used, corresponding to changes of cell edges in the range ±0.13 Å. The usual polynomial interpolations yielded $C_{11}+C_{12}$ and $C_{11}-C_{12}$, whence C_{11} and C_{12} which are reported in table 3. The corresponding value of the bulk modulus, $B = (C_{11} + 2C_{12})/3$, is 83.1 GPa in good agreement with 82.6 derived independently by the Murnaghan fit to the $[\eta\ \ \eta\ \ \eta\ \ 0\ \ 0\ \ 0]$ deformation. A very good agreement with both experimental results is observed for the computed C_{11} value. C_{12} shows a substantial deviation from the ultrasonic data, but agrees well with the Brillouin scattering result.

In order to calculate the shear elastic constant C_{44}, the $[0\ \ 0\ \ 0\ \ \eta\ \ \eta\ \ \eta]$ lattice strain was considered, corresponding to a rhombohedral deformation of the cubic unit cell. The α, β, γ angles increase ($\eta < 0$) or decrease ($\eta > 0$) by the same quantity, according to a compression or a stretching along the [1 1 1] diagonal, respectively. Substituting into (3), the derivative $\mathrm{d}^2E/\mathrm{d}\eta^2$ gives $C_{44} + C_{55} + C_{66}$ in this case, so it must be divided by three. Ten η values, ranging between -0.10 and $+0.10$, were used. A value of 48.0 GPa was obtained for C_{44}, which is larger than the experimental ones by nearly 30%. However, this calculation neglects the inner strain of the fluorine atom, which acquires a positional degree of freedom along the cube diagonal transformed into the rhombohedral axis by the symmetry lowering (Srinavasan 1968). The overestimation of elastic constants when internal deformations are not taken into account is a well known effect (Catti 1985, Catti 1989). Let us denote by u the shift of F along the threefold axis due to a strain η; correspondingly, a correction term $E_1(u,\eta)$ has to be added to the energy of the unrelaxed configuration $E_0(\eta)$, so that the total energy is $E(u,\eta) = E_0(\eta) + E_1(u,\eta)$. The condition of minimum E, $(\partial E_1/\partial u)_\eta = 0$, gives the inner strain $u = u(\eta)$, and by substitution the energies $E_1(\eta)$ and $E(\eta)$ are obtained as functions of η only. The problem could be solved numerically by minimizing the quantity $E_1(u,\eta)$ with respect to u for each of the η values considered; however, to reduce the computing time this procedure was limited to some of the η values only, and then by a least-squares polynomial interpolation the complete $u(\eta)$ and $E_1(\eta)$ curves were built up (figure 2). As expected, the inner strain effect is much stronger on the negative (compression) than on the positive (dilatation) side of the η axis, where it appears nearly negligible. In the first case, the $E_1(\eta)$ data were fitted by a cubic parabola with coefficient 3.448 hartree, while the $u(\eta)$ interpolation function is $-0.5281\eta + 4.3448\eta^2$ (Å). Pairs of F atoms lying on the threefold axis separate for $\eta < 0$ and approach for $\eta > 0$. By using the total energy $E(\eta)$ instead of the pure lattice strain term $E_0(\eta)$, the value of C_{44} including inner strain contribution was reduced to 44 GPa, thus remaining significantly larger than the experimental results (table 3).

It is well known (Hehre *et al* 1986) that the HF approximation simulates longer and stiffer interatomic bonds, so that obtaining larger elastic constants as for C_{44} is not surprising. On the other hand, the C_{11}, C_{12} and B values are all smaller than those measured. This is due to use of the larger calculated unit-cell edge, which produces a less rigid crystal according to the $B(V)$ curve, with an overcompensation for the HF error. Such an effect is not observed for C_{44} because of the very small volume dependence of shear elastic components.

The vibrational frequencies of two transverse optical modes at the centre of the Brillouin zone (Elcombe and Pryor 1970), IR and Raman active, respectively, were also calculated. As the modes are threefold degenerate in x, y, z, the linear combination corresponding to a motion along the cube diagonal could be used. Appropriate shifts were applied to F atoms in the unit cell, and the energy was computed for deformed configurations as a function of the atomic displacement u. In the Raman active mode, two fluorines vibrate along the diagonal against the fixed Ca atom at (0,0,0), shifting to positions $(\frac{1}{4}+\delta, \frac{1}{4}+\delta, \frac{1}{4}+\delta)$ and $(-\frac{1}{4}-\delta, -\frac{1}{4}-\delta, -\frac{1}{4}-\delta)$, respectively. The normal coordinate is $u = 2\sqrt{3}\delta$, corresponding to the variation of the F–F distance, and the reduced mass is $M = m_\mathrm{F}/2$. In the IR active mode the two F atoms vibrate in-phase, so that they were given the same displacement δ; the normal coordinate is $u = \sqrt{3}\delta$ (i.e. the change in the F–Ca distance), and the reduced mass is $M = 2m_\mathrm{F}m_\mathrm{Ca}/(2m_\mathrm{F}+m_\mathrm{Ca})$ in this case. By the usual polynomial fits of E again u, the harmonic force constants

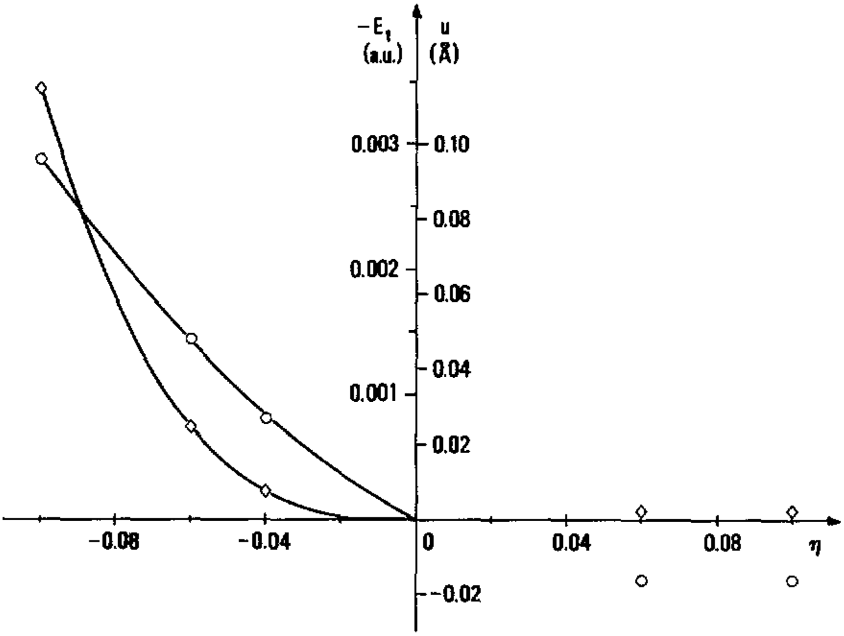

Figure 2. Inner strain contribution E_I to energy (circles), and corresponding shift u of the F atom (diamonds), as functions of the rhombohedral deformation component η in the calculation of the elastic constant C_{44}.

K could be derived as $\mathrm{d}^2E/\mathrm{d}u^2$, and the corresponding frequencies were given simply by $\nu = (K/M)^{1/2}$. If atomic units are used for E, u and M, then multiplication by 154.1079 is required to obtain ν in THz. The computed values of ν(IR) and ν(Raman) are reported in table 3 and compared with experimental results (Lowndes 1971 and Denham *et al* 1970, respectively) extrapolated to the athermal limit. Agreement is very satisfactory.

5. Electron band structure, density of states and charge density

The band structure of $\mathrm{CaF_2}$ is shown in figure 3. As expected for an ionic crystal, the bands are very flat and separated by large gaps. The energy gap-width between valence and conduction bands at the Γ point is about 21 eV, to be compared with 12 eV from experiment (Poole *et al* 1975). A very well known effect of the HF Hamiltonian is to overestimate the energy gaps; in this case the error is even larger since the adopted basis set, though quite accurate for representing the ground state, describes the lowest excited states poorly (in particular because no diffuse valence orbitals on Ca are included). Previous energy band calculations on fluorite were performed by Evarestov *et al* (1989), who used the CNDO semi-empirical approximation in the frame of a SCF-HF treatment, and by Albert *et al* (1977), who employed a tight binding scheme. In the first work an energy gap in the range from 13.6 to 14.4 eV was computed, in much better agreement with experiment than our result. This would indicate a partial compensation between the intrinsic error of the HF scheme and that of the CNDO approximation.

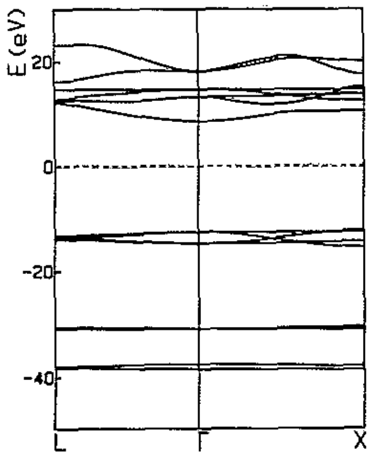

Figure 3. Electronic band structure of CaF_2 along symmetry lines; valence and conduction bands, separated by the broken line, are shown.

A Mulliken electron population analysis confirms the ionic nature of chemical bonding in CaF_2: the net charge on Ca ($+1.868|e|$) is close to the formal ionic value $+2|e|$, and a very low Ca–F bond population ($-0.008|e|$) is observed. In this respect, it is interesting to consider the detailed ion charge distribution and, in particular, its modifications brought about by isotropic compression (table 4). For a decrease of 5% of the cell edge a from 5.403 to 5.170 Å, the Ca total electron charge increases by $-0.033|e|$, and the net charge lowers to $+1.835|e|$, indicating a tendency to less ionic bonding. The extra negative charge is entirely located on the d shell ($-0.043|e|$); the sp electron cloud contracts, and $-0.015|e|$ of the 4sp and 5sp shells are transferred partially to the inner 3p shell and to the d orbitals. A similar electron flow from the outer 4sp to the inner 3sp and 2sp shells is observed for fluorine, in addition to the electron transfer to the d orbitals of Ca.

Table 4. Effects of isotropic compression of the cell edge a (Å) on the shell charges ($|e|$) of Ca and F, which are evaluated according to the Mulliken partition scheme. Shell symbols refer to table 1.

a		5.463	5.310	5.170
Ca	2sp	−8.078	−8.077	−8.077
	3sp	−4.562	−4.567	−4.568
	4sp	−2.519	−2.508	−2.509
	5sp	−0.870	−0.873	−0.865
	d	−0.103	−0.124	−0.146
	total	−18.132	−18.150	−18.165
F	2sp	−3.933	−3.940	−3.948
	3sp	−2.898	−2.916	−2.929
	4sp	−1.103	−1.070	−1.041
	total	−9.934	−9.925	−9.918

In figure 4, the total and projected densities of electron states are reported. The occupied bands appear to be nearly pure atomic-like states, with no mixed contributions except perhaps for a very small overlap of d(Ca) ($q_d = 0.103e$, not appearing in the figure) with the p(F) orbitals in the valence band. On the other hand, the d orbitals of Ca were previously shown to have an appreciable effect on lattice and elastic properties of fluorite. The conduction band is contributed mainly by d(Ca) and p(F) states, with a minor role for p(Ca) and s(F) orbitals; this contrasts with the results of Evarestov *et al* (1989), which show major contributions from s(Ca) and s(F) orbitals.

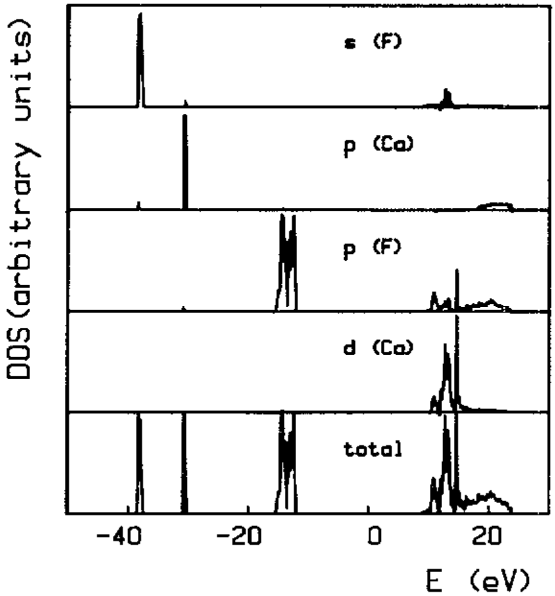

Figure 4. Projected and total density of states of CaF_2. The atomic orbital contributions have been obtained using a Mulliken partition scheme.

Total and difference (= total crystal minus ionic superposition) electron density maps were computed on the (110) plane, limited to a portion comprising two Ca and two F atoms, and are shown in figures 5 and 6, respectively. A contraction of electron clouds in the crystal with respect to the free ion state appears clearly, and is due both to electron exchange repulsion (Pauli's exclusion principle) and to the compression effect of the crystal electrostatic field for the anions. In figure 7, the contribution of d orbitals of Ca to the total electron density of CaF_2 is shown. Positive isodensity lines around Ca atoms are observed and can be ascribed to slightly populated d orbitals; negative lines close to F atoms, on the other hand, are due to a small charge transfer to d(Ca) states and consequent depopulation of p(F) orbitals, in agreement with density-of-states analysis.

6. Conclusions

The present work represents the first attempt to compute the complete elastic tensor of an ionic solid (CaF_2) by means of the *ab inititio* LCAO-HF model, and has met with reasonable success. The importance of allowing for inner strain effects has been demonstrated by almost a 10% reduction in C_{44} after such allowance. Even so, the calculations give C_{44} slightly larger than C_{12}, whereas experimentally the opposite

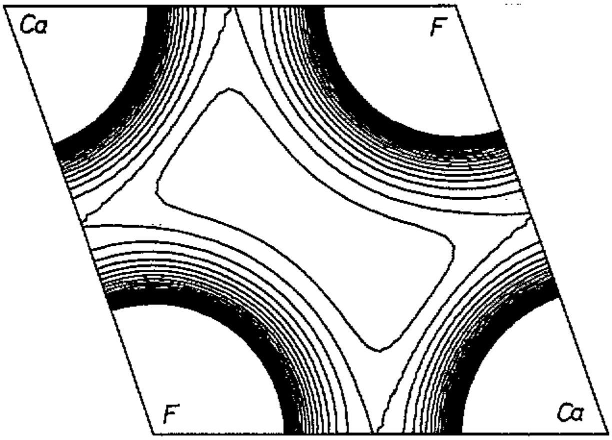

Figure 5. Total electron density map on the (110) plane through Ca and F atoms. The separation between isodensity curves is 0.01e Bohr^{-3}.

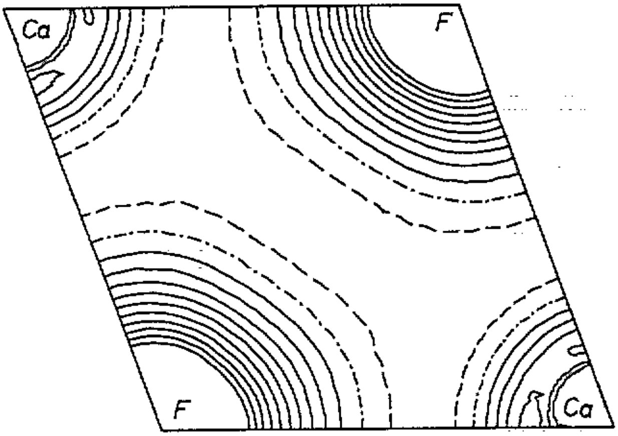

Figure 6. Difference (crystal minus ionic superposition) electron density map on the (110) plane. Continuous, chain and broken lines indicate positive, zero and negative values, respectively. The separation between isodensity curves is 0.001e Bohr^{-3}.

is the case. The computed lattice constants are found to be 1.7% too large, whilst excellent agreement is found for the central zone transverse optic mode phonon frequencies and for the BE (after allowance for the difference between isolated atom and ion correlation energies). The calculations are consistent with a highly ionic model of the crystal, as indicated by a Mulliken population analysis and the projected density of states.

Crystal formation is accompanied by contraction of both the anion and cation, a result is qualitative agreement with the breathing shell model (Woods *et al* 1960, Schröder 1966, Nusslein and Schröder 1967), but in disagreement with the potential induced breathing model, which predicts that the cation should expand under influence of the crystalline Madelung potential.

Under compression, a further contraction of the ions is apparent,and also a charge transfer from the fluorine valence p orbitals to the Ca d shell, indicating an important contribution of such d orbitals to crystal stability. Indeed, if the calculations are

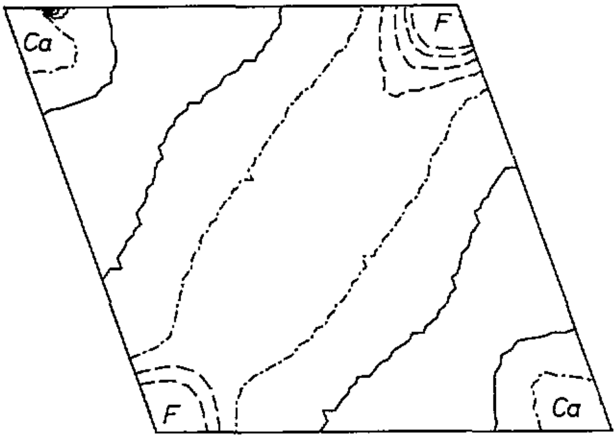

Figure 7. Effect of d orbitals on the electron charge density. The difference between the electron charge density obtained with and without d orbitals on calcium, on the (110) plane, is shown. Symbols and scale as in figure 6.

repeated without the Ca d shell, the predicted equilibrium lattice constant increases by 0.063 Å to 5.601 Å, while the BE is decreased by 0.017 Hartree/cell.

Acknowledgments

This work was supported financially by CSI Piemonte (Turin) and by the Ministero Universita' e Ricerca Scientifica e Tecnologica (Rome).

References

Albert J P, Jouanin C and Gout C 1977 *Phys. Rev.* B **16** 4619–29
Basu A N and Sengupta S 1968 *Phys. Status Solidi* **29** 367–75
Born M and Huang K 1954 *Dynamical Theory of Crystal Lattices* (London: Oxford University Press)
Catlow C R A and Norgett M J 1973 *J. Phys. C: Solid State Phys.* **6** 1325–39
Catlow C R A, Comins J D, Germano F A, Harley R T and Hayes W 1978 *J. Phys. C: Solid State Phys.* **11** 3197–213
Catti M 1982 *J. Phys. Chem. Solids* **43** 1111–8
—— 1985 *Acta Crystallogr.* A **41** 494–500
—— 1989 *Acta Crystallogr.* A **45** 20–5
Causa' M, Dovesi R, Pisani C and Roetti C 1986 *Phys. Rev.* B **33** 1308–16
Chen J, Boyer L L, Krakauer H and Mehl M J 1988 *Phys. Rev.* B **37** 3295–8
Chang K S and Cohen M L 1984 *Phys. Rev.* B **30** 4774–81
Christensen N E 1986 *Phys. Rev.* B **33** 5096–8
Clementi E 1963 *J. Chem. Phys.* **38** 2248–56
Cohen A J and Gordon R G 1976 *Phys. Rev.* B **14** 4593–605
Cohen R E, Boyer L L and Mehl M J 1987 *Phys. Rev.* B **35** 5749–60
Denham P, Field G R, Morse P L R and Wilkinson G R 1970 *Proc. R. Soc.* A **317** 55–77
Dick G B and Overhauser A W 1958 *Phys. Rev.* **112** 90–103
Dovesi R 1984 *Int. J. Quantum Chem.* **26** 197–212
Dovesi R, Ermondi C, Ferrero E, Pisani C and Roetti C 1984a *Phys. Rev.* B **30** 3591–600
Dovesi R, Pisani C, Ricca F, Roetti C and Saunders V R 1984b *Phys. Rev.* B **30** 972–9
Dovesi R, Pisani C, Roetti C, Causa' M and Saunders V R 1989 *Crystal 88. Quantum Chemistry Program Exchange (Indiana University, Bloomington, IN, 1989) Program No* 577

Elcombe M M and Pryor A W 1970 *J. Phys. C: Solid State Phys.* **3** 492–9
Evarestov R A, Murin I V and Petrov A V 1989 *J. Phys.: Condens. Matter* **1** 6603–9
Feldman J L, Mehl M J and Krakauer H 1987 *Phys. Rev.* B **35** 6395–8
Feldman J L, Mehl M J, Boyer L L and Chen N C 1988 *Phys. Rev.* B **37** 4784–7
Fischer K 1974 *Phys. Status Solidi* b **66** 295–304
Fischer K, Bilz H, Haberkorn R and Weber W 1972 *Phys. Status Solidi* b **54** 285–94
Froyen S and Cohen M L 1984 *Phys. Rev.* B **29** 3770–2
Garber J A and Granato A V 1975a *Phys. Rev.* B **11** 3990–7
—— 1975b *Phys. Rev.* B **11** 3998–4007
Gordon R G and Kim Y S 1972 *J. Chem. Phys.* **56** 3122–33
Harries H J and Morris D F C 1959 *Acta Crystallogr.* **12** 657–9
Hemley R J, Jackson M D and Gordon R G 1985 *Geophys. Res. Lett.* **12** 247–50
Hehre W H, Radom L, Schleyer P R and Pople J A 1986 *Ab initio Molecular Orbital Theory* (New York: Wiley)
Ho P S and Ruoff A L 1967 *Phys. Rev.* **161** 864–9
Jephcoat A P, Hemley R J, Mao H K, Cohen R E and Mehl M J 1988 *Phys. Rev.* B **37** 4727–34
Liebfried G and Ludwig W 1961 *Solid State Physics* **12** 275–444
Lowndes R P 1971 *J. Phys. C: Solid State Phys.* **3** 3083–94
Mehl M J, Hemley R J and Boyer L L 1986 *Phys. Rev.* B **33** 8685–96
Mehl M J, Cohen R E and Krakauer H 1988 *J. Geophys. Res.* **93** 8009–22
Melvin J S and Hendry D C 1982 *J. Phys. C: Solid State Phys.* **15** 2093–103
Muhlhauser C and Gordon R 1981a *Phys. Rev.* B **23** 900–23
—— 1981b *Phys. Rev.* B **24** 2147–59
Murnaghan F D 1944 *Proc. Nat. Acad. Sci. USA* **30** 244–7
Nusslein V and Schröder U 1967 *Phys. Status Solidi* **21** 309–14
Orlando R, Dovesi R, Roetti C and Saunders V R 1990 *J. Phys.: Condens. Matter* **2** 7769–89
Pisani C, Dovesi R and Roetti C 1988 *Hartree–Fock Ab Initio Treatment of Crystalline Solids (Lecture Notes in Chemistry Series 48)* (Berlin: Springer)
Poole R T, Szajman J, Leckey R C G, Jenkin J G and Liesegang J 1975 *Phys. Rev.* B **12** 5872–7
Schröder U 1966 *Solid State Commun.* **4** 347–9
Srinivasan R 1968 *Phys. Rev.* **165** 1054–62
Straub G K and Harrison W A 1989 *Phys. Rev.* B **39** 10325–30
Weast R C (ed) 1987 *Handbook of Chemistry and Physics* (Boca Raton, USA: Chemical Rubber Company)
White G K 1980 *J. Phys. C: Solid State Phys.* **13** 4905–13
Woods A D B, Cochran W and Brockhouse B N 1960 *Phys. Rev.* **119** 980–99
Wyckoff W G 1968 *Crystal Structures* vol 1, 2nd edn (New York: Wiley)